



circ_0000337 Promotes the Progression of Cervical Cancer by miR-155-5p/RAB3B Axis

Jiqin Xu¹ · Bai Xue¹ · Min Gong¹ · Ling Ling¹ · Sipei Nie¹ · Fujun Li¹ · Meixia Wang² · Miao Fang¹ · Chen Chen³ · Qiaoling Liu¹ · Yun Han^{3,4}

Received: 14 July 2023 / Accepted: 22 September 2023

© The Author(s), under exclusive licence to Springer Science+Business Media, LLC, part of Springer Nature 2023

Abstract

Current study aims to investigate the biological function of circular RNA (circRNA, circ_0000337) in cervical cancer (CC). Bioinformatic analyses were used to predict targets for circ_0000337 and miR-155-5p, and analyze the gene expression differences between cervical squamous cell carcinoma and endocervical adenocarcinoma (CESC) tissues and normal tissues. Quantitative real-time polymerase chain reaction (qRT-PCR) and Western blot were applied to assess mRNA and protein expressions of circ_0000337, microRNA-155-5p (miR-155-5p) and member RAS oncogene family (RAB3B), respectively. Following the establishment of gain/loss-of-function models, CCK-8 was performed to evaluate cell proliferation. Bioinformatics analysis, dual-luciferase reporter assay and RNA immunoprecipitation (RIP) were used to identify the interaction in circ_0000337, miR-155-5p, and RAB3B. Circ_0000337 and RAB3B were upregulated, while miR-155-5p was downregulated in CC tissues and cell lines. circ_0000337 overexpression promoted cell proliferation, circ_0000337 knock down inhibited cell proliferation by sponging miR-155-5p. RAB3B was a target of miR-155-5p which was positively regulated by circ_0000337. In the collected CC tissues, there was a negative correlation between miR-155-5p and circ_0000337 or RAB3B, and a positive correlation between circ_0000337 and RAB3B. miR-155-5p was positively, while RAB3B was negatively correlated with OS in patients with CC, and they were negatively correlated. In conclusion, circ_0000337 upregulates RAB3B by sponging miR-155-5p to promote CC cell proliferation.

Keywords Cervical Cancer · circ_0000337 · miR-155-5p · RAB3B

Introduction

Cervical cancer (CC) is the second leading cause of cancer-related deaths in females who aged about 20–39 years old (Siegel et al. 2019). Hysterectomy exerts the most effective effect on long-term survival, meanwhile, it is the primary choice for the treatment of early-stage CC (Fader 2018). Despite radiotherapy shows superiority in therapy-related toxicity for patients with locally-advanced CC (Cohen et al. 2019), those who suffer with invasive CC still undergo a risk of secondary malignancies (Jhamad et al. 2018). Recently, novel therapeutic targets have attracted more and more attentions according to comprehensive genomic characteristics of CC (Cancer Genome Atlas Research Network et al. 2017).

Circular RNAs (circRNAs) are a subgroup of non-coding RNAs produced from precursor mRNA back-splicing of various genes in eukaryotes which expressed in a cell-specific or tissue-specific manner (Chen 2016). CircRNAs are implicated in numerous human diseases (Han et al. 2018), and serve as potential oncogenes or tumor suppressors in human cancers (Chen and Huang 2018). Specifically, mounting circRNAs are dysregulated in CC tissues compared to normal tissues (Li et al. 2019). Functionally, circRNAs act as sponges or competing endogenous RNAs (ceRNA) for microRNAs (miRNAs or miRs) to regulate mRNA expression (Jeck and Sharpless 2014; Arnaiz et al. 2019), for instance, circ_0000337 promotes cell proliferation, migration, and invasion of esophageal squamous cell carcinoma (Song et al. 2019), circ_0000337 contributes to proliferation and migration of osteosarcoma by miR-4458/BACH1 (Fang and Long 2020), circ_0000337 promotes proliferation, migration and invasion in glioma by miR-942-5p/MAT2A (Liu et al. 2020), exosomes mediated transfer of circ_0000337 enhances cisplatin resistance of esophageal cancer by miR-377-3p/JAK2 (Zang et al. 2021).

MiRNAs are a subgroup of short noncoding RNAs with approximately 21 nucleotides, which show crucial effects on CC (Wilting et al. 2013). Numerous miRNAs serve as oncogenes such as miR-1908 (Yu et al. 2021), and many miRNAs act as tumor suppressors like miR-532-5p (Shang et al. 2021). Nonetheless, the exact relation between circ_0000337 and miRNAs in CC is largely unknown.

Current study focuses on the implication of circ_0000337 in CC, which is proved to be associated with miR-155-5p and RAB3B. Altogether, the findings indicate the circ_0000337/miR-155-5p/RAB3B network in the carcinogenesis of CC, and highlight potential novel targets for the treatment of CC.

Materials and Methods

Study Subjects

A total of 23 patients diagnosed with CC were enrolled in the Affiliated Hospital 2 of Nantong University. Patients with CC (aged 49.05 ± 10.04 years old) underwent surgical treatment in Affiliated Hospital 2 of Nantong University from Jan,

2018 to Feb, 2022. None of them received any drug treatment or distant metastasis prior to surgery. Normal mucosal tissues 2 cm away from cancer tissues were extracted. Tissues were stored at -80°C immediately. Current study is approved by the Ethics Committee of Affiliated Hospital 2 of Nantong University. All patients signed informed consent before the enrollment.

Bioinformatic Analysis

ENCORI software (<http://starbase.sysu.edu.cn/index.php>) was used for the analysis of miRNA targets for circ_0000337. TargetScan V7.2 (http://www.targetscan.org/vert_72/) software was adopted for the analysis of mRNA targets for miR-155-5p. The RAB3B expression differences between cervical squamous cell carcinoma and endocervical adenocarcinoma (CESC) tissues and normal tissues were analyzed by ENCORI software (<http://starbase.sysu.edu.cn/index.php>) based on TCGA datasets, GEPIA (<http://gepia.cancer-pku.cn/>), and Kaplan-Meier Plotter (<http://kmplot.com/analysis/index.php?p=service>). The miR-155-5p expression differences between CESC tissues and normal tissues were analyzed by UALCAN database (<http://ualcan.path.uab.edu/index.html>) and Kaplan-Meier Plotter (<http://kmplot.com/analysis/index.php?p=service>). The correlation between RAB3B and miR-155-5p was studied by ENCORI software (<http://starbase.sysu.edu.cn/index.php>) based on TCGA dataset.

Cell Culture

CC cell lines (Hela, SiHa, C33A) and normal cervical epithelial cells H8 were purchased from the Chinese Academy of Medical Sciences (Beijing, China). Cells were cultured in RPMI-1640 medium (Invitrogen, Carlsbad, CA, USA) supplemented with 10% fetal bovine serum (FBS, Gibco, Grand Island, NY, USA), 100 $\mu\text{g}/\text{ml}$ streptomycin, and 100 U/ml penicillin (Hyclone, Logan, UT, USA). Next, cells were incubated in an incubator with 5% CO_2 at 37°C .

Cell Transfection

Cells (3×10^5 cells/well) were plated into a 6-well plate. Thereafter, HeLa cells were co-transfected with pcDNA3.1 (negative control, NC group), pcDNA3.1-circ_0000337 (circ_0000337 group), and miR-negative control (NC) mimic or miR-155-5p mimic, while C33A cells were co-transfected with si-NC, siRNA targeting circ_0000337 (si-circ-0000337 group), and miR-NC inhibitor or miR-155-5p inhibitor (GenePharma, Shanghai, China) by Lipofectamine® 3000 (Invitrogen, Carlsbad, CA, USA). At last, cells were harvested at 48 h after transfection.

Quantitative Real-time Polymerase Chain Reaction

Total RNA was extracted by Trizol (Invitrogen). Afterwards, RNA was reverse transcribed into cDNA by Primescript™ RT reagent (TaKaRa, Dalian, China).

Reverse transcription of miR-155-5p and U6 was performed by Mir-X™ miRNA First-Strand Synthesis kit (Clontech, USA). cDNA was subjected to qRT-PCR with SYBR® Premix Ex Taq™ II Kit (TaKaRa, Dalian, China), and conducted in an ABI PRISM® 7300 system (ABI, USA). U6 and GAPDH served as the references for miR-155-5p and genes including circ_0000337 and RAB3B, respectively. Primers were listed in Table 1. Relative gene expression was analyzed by $2^{-\Delta\Delta C_t}$ method (Schefe et al. 2006).

Western Blot

Total protein from tissues and cells was extracted by radioimmunoprecipitation assay (RIPA) lysis buffer containing phenylmethanesulfonyl fluoride (PMSF). Samples were separated by sodium dodecyl sulfate-polyacrylamide gel electrophoresis (SDS-PAGE), and transferred onto the polyvinylidene difluoride (PVDF) membrane. After being blocked by 5% skim milk for 1 h at room temperature, the PVDF membranes were incubated with rabbit antibodies against human RAB3B (25 kD, ab235518, 1: 2000, Abcam), and GAPDH (37 kD, ab9485, 1: 3000, Abcam) at 4 °C overnight. On the next day, the PVDF membrane was incubated with horseradish peroxidase (HRP)-labeled goat anti-rabbit immunoglobulin G (IgG) secondary antibody (ab6721, 1: 2000, Abcam) at room temperature for 2 h. Then, the PVDF membranes were developed by an enhanced chemiluminescence (ECL) kit (Ameshame, UK), and captured by a Bio-Rad image analysis system (Bio-Rad, Hercules, CA, USA). Finally, the band intensity was analyzed by Quantity One (version 4.6.2).

Table 1 Association between circ_0000337 and clinicopathological features of CC

Characteristics	Patient numbers (n = 23)	circ_0000337 expression		<i>p</i>
		Low (n = 11)	High (n = 12)	
Age (years)				
< 40	12	7	5	0.263
≥ 40	11	4	7	
Tumor size (cm)				
< 4	11	8	3	0.030
≥ 4	12	3	9	
HPV infection				
Positive	14	6	8	0.433
Negative	9	5	4	
Differentiation				
Low, moderate	13	9	4	0.026
High	10	2	8	

Cell Proliferation

Cells were inoculated into a 96- well plate (2×10^3 cells/well) and incubated for 24 h in an incubator with 5% CO₂ at 37 °C. Afterwards, 10 µl of cell counting kit8 (CCK-8) (MedChemExpress, Monmouth Junction, NJ, USA) was added into each well and incubated for another 1 h in an incubator with 5% CO₂ at 37 °C. The absorbance (OD 450 nm) of each well was recorded by a Bio-Tek Synergy HT Microplate Reader (Bio-Tek Instruments, Winooski, VT, USA).

Dual-Luciferase Reporter Assay

The dual-luciferase reporter assay system (Promega, Madison, WI, USA) was used to detect the relative luciferase activity. Cells were inoculated in a 24-well plate (1×10^4 cells/well) and cultured for 24 h in an incubator with 5% CO₂ at 37 °C. When cell confluence reached 80–90%, the transfection was performed by Lipofectamine® 3000 (Invitrogen). Wild-type circ_0000337 (WT circ_0000337), wild-type RAB3B (WT RAB3B), mutant-type circ_0000337 (MUT circ_0000337) and mutant-type RAB3B (MUT RAB3B) reporter vectors were co-transfected with mimic NC or miR-155-5p mimic, respectively. After being cultured for 48 h in an incubator with 5% CO₂ at 37 °C, cells were harvested. After that, the luciferase substrate was added, firefly luciferase activity was examined by the luminometer (Promega, Madison, WI, USA). Renilla luciferase activity served as the internal reference.

RNA Immunoprecipitation Assay

The interaction between circ_0000337 and miR-155-5p was determined by Magna RIP™ RNA-Binding Protein Immunoprecipitation Kit (Millipore, Billerica, MA, USA). Cells were lysed in the RIP lysis buffer, cell lysates (100 µl) were incubated with magnetic beads coupling with anti-Argonaute2 (Ago2) antibody or IgG (NC) in the RIP buffer. Samples were incubated with Proteinase K (Invitrogen) to remove proteins, then RNA precipitation was collected. The purified RNA was subjected to qRT-PCR as aforementioned.

Statistical Analysis

GraphPad software (version 6.0, GraphPad, USA) was utilized for statistical analysis. Each experiment was conducted thrice independently. Data were expressed as mean \pm standard deviation. The paired data between two groups were analyzed by paired student's t test, while unpaired data between two groups were analyzed by unpaired student's t test. Data comparisons between multiple groups were conducted by one-way analysis of variance (ANOVA) with Tukey's post hoc test. The correlation between miR-155-5p or RAB3B and OS in

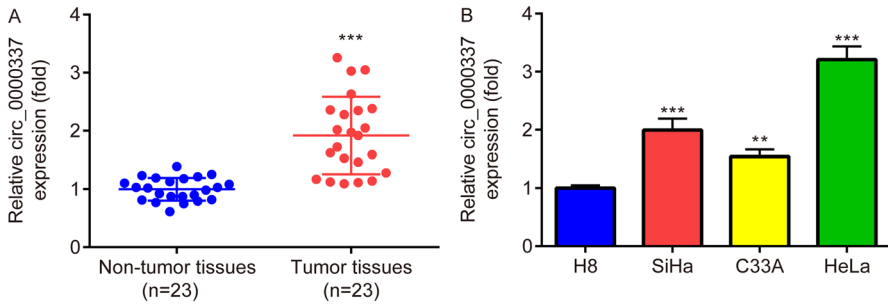


Fig. 1 circ_0000337 is upregulated in CC tissues and cells. circ_0000337 is increased in CC tissues (A) and cell lines (B) in contrast to the adjacent non-cancerous tissues and H8, respectively. ** $p < 0.01$ vs. H8, *** $p < 0.001$ vs. non-tumor tissues, H8

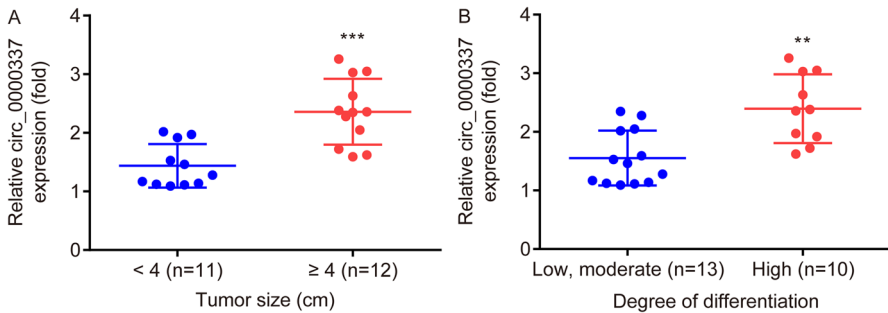


Fig. 2 circ_0000337 is correlated with tumor size and differentiation of CC tissues. High circ_0000337 expression is correlated with large tumor size (A) and high differentiation of CC tissues (B). ** $p < 0.01$ vs. low, moderate differentiation, *** $p < 0.001$ vs. tumor size < 4 cm

patients with CC was analyzed by Pearson correlation analysis. $P < 0.05$ indicated statistical significance.

Results

circ_0000337 is Upregulated in CC Tissues and Cells

circ_0000337 is increased in CC tissues in contrast to the adjacent non-cancerous tissues (Fig. 1A). In addition, circ_0000337 is increased in CC cell lines (SiHa, HeLa, C33A) compared with normal cervical epithelial cell line H8 (Fig. 1B). Collectively, the findings suggest the involvement of circ_0000337 in the progression of CC.

circ_0000337 is Correlated with Tumor Size and Differentiation of CC Tissues

By analyzing the correlation between circ_0000337 and clinical characteristics, it is discovered that high circ_0000337 expression is correlated with large tumor size

(Fig. 2A) and high differentiation of CC tissues (Fig. 2B), but not age or HPV infection (Table 1). The results demonstrate that circ_0000337 may be involved in tumor growth of CC.

circ_0000337 Facilitates Cell Proliferation of CC

C33A cells with the lowest circ_0000337 are transfected with pcDNA3.1-circ_0000337 (Fig. 3A), while HeLa cells with the highest circ_0000337 are transfected with si-circ_0000337 (Fig. 3B).

circ_0000337 overexpression facilitates C33A cell proliferation (Fig. 3C), while circ_0000337 knock down represses HeLa cell proliferation (Fig. 3D). The results demonstrate that circ_0000337 is involved in cell proliferation of CC.

circ_0000337 Directly Targets miR-155-5p

miR-155-5p is predicted as a one of the target miRNAs for circ_0000337 (Fig. 4A). Dual-luciferase reporter assay indicates that miR-155-5p mimic represses the luciferase activity of WT circ_0000337 but not MUT circ_0000337 in C33A (Fig. 4B) and HeLa (Fig. 4C). Subsequently, RIP assay demonstrates that circ_0000337 and miR-155-5p are enriched in the Ago2-containing microribonucleoproteins in contrast to IgG in C33A (Fig. 4D) and HeLa (Fig. 4E), suggesting a direct interaction between circ_0000337 and miR-155-5p.

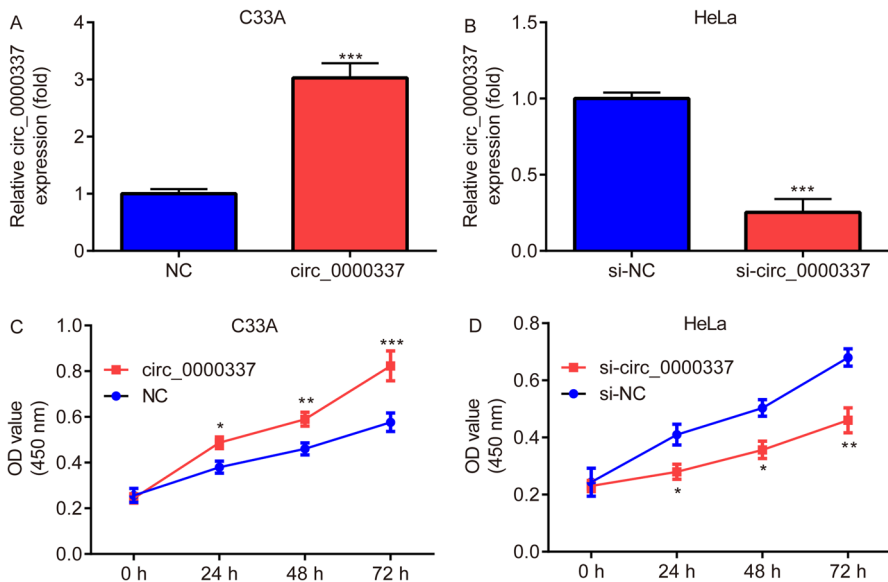


Fig. 3 circ_0000337 facilitates cell proliferation of CC. C33A cells are transfected with pcDNA3.1-circ_0000337 (A), while HeLa cells are transfected with si-circ_0000337 (B). circ_0000337 overexpression facilitates C33A cell proliferation (C), while circ_0000337 knock down represses HeLa cell proliferation (D). * $p < 0.05$, ** $p < 0.01$, *** $p < 0.001$ vs. NC, si-NC

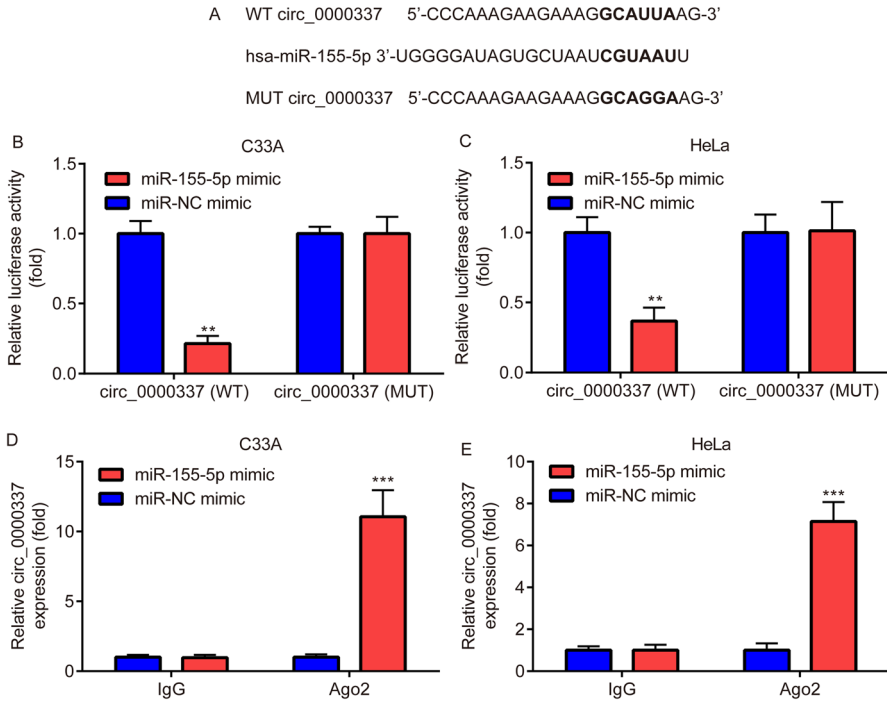


Fig. 4 circ_0000337 directly targets miR-155-5p. miR-155-5p is predicted as a one of the target miRNAs of circ_0000337 (A). miR-155-5p mimic represses the luciferase activity of WT circ_0000337 but not MUT circ_0000337 in C33A (B) and HeLa (C). circ_0000337 and miR-155-5p are enriched in the Ago2-containing microribonucleoproteins in contrast to IgG in C33A (D) and HeLa (E). ** $p < 0.01$, *** $p < 0.001$ vs. miR-NC mimic

circ_0000337 is Inversely Correlated with miR-155-5p

The downregulated expression of miR-155-5p is found in CC cell lines relative to H8 (Fig. 5A). Meanwhile, miR-155-5p is diminished in CC tissues compared with the adjacent non-cancerous tissues (Fig. 5B). Pearson's correlation analysis indicates that circ_0000337 is negatively correlated with miR-155-5p expression in the collected CC tissues (Fig. 5C). Altogether, there is an inverse correlation between circ_0000337 and miR-155-5p, suggesting the inverse roles of circ_0000337 and miR-155-5p in CC.

circ_0000337 Facilitates Cell Proliferation of CC by Sponging miR-155-5p

pcDNA3.1-circ_0000337 and miR-155-5p mimic are co-transfected into C33A cells, exhibiting that pcDNA3.1-circ_0000337-induced downregulation of miR-155-5p level is rescued by miR-155-5p mimic (Fig. 6A), while si-circ_0000337 and miR-155-5p inhibitor are co-transfected into HeLa cells, exerting that

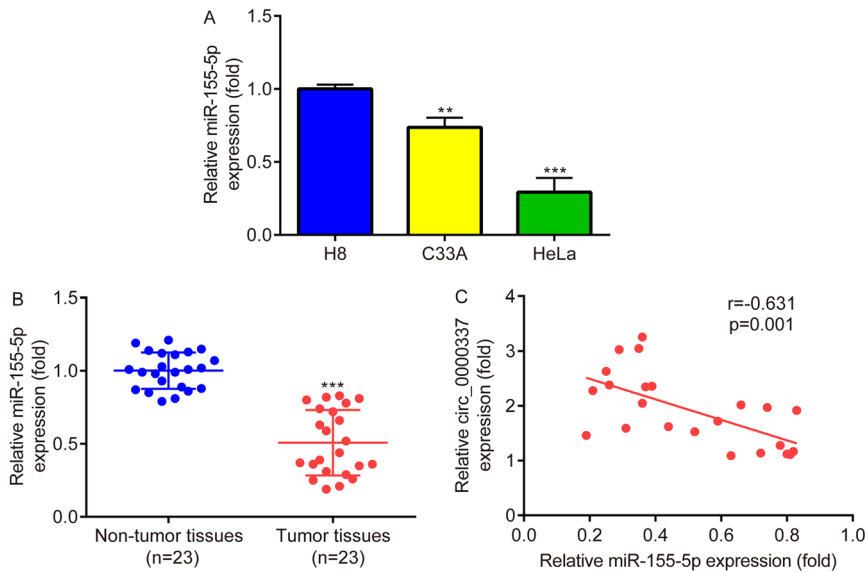


Fig. 5 circ_0000337 is inversely correlated with miR-155-5p. The downregulated expression of miR-155-5p is found in CC cell lines (A) and tumor tissues (B) relative to H8 and the adjacent non-cancerous tissues, respectively. circ_0000337 is negatively correlated with miR-155-5p in the collected CC tissues (C). ** $p < 0.01$ vs. H8, *** $p < 0.001$ vs. non-tumor tissues, H8

si-circ_0000337-induced upregulation of miR-155-5p level is attenuated by miR-155-5p inhibitor (Fig. 6B).

pcDNA3.1-circ_0000337-induced facilitation of C33A cell proliferation is attenuated by miR-155-5p mimic (Fig. 6C), si-circ_0000337-induced repression of HeLa cell proliferation is partially reversed by miR-155-5p inhibitor (Fig. 6D). Taken together, the promotive effects of circ_0000337 in cell proliferation of CC are realized by sponging miR-155-5p.

circ_0000337 Upregulates RAB3B Expression by Targeting miR-155-5p

RAB3B is predicted as one of the potential mRNA targets for miR-155-5p (Fig. 7A). Dual-luciferase reporter assay exerts that miR-155-5p mimic diminishes the luciferase activity of WT RAB3B but not MUT RAB3B in C33A (Fig. 7B) and HeLa (Fig. 7C).

Western blot shows that circ_0000337 overexpression enhances RAB3B expression in C33A cells, which is attenuated by miR-155-5p mimic (Fig. 7D and E), circ_0000337 knock down impedes RAB3B expression in HeLa cells, which is counteracted by miR-155-5p inhibitor (Fig. 7D and F). In conclusion, circ_0000337 increases RAB3B expression by sponging miR-155-5p.

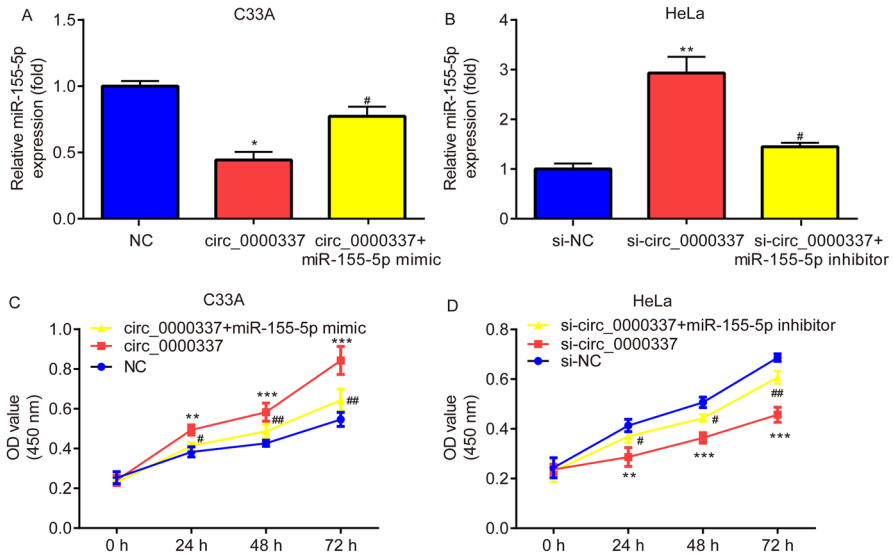


Fig. 6 circ_0000337 facilitates cell proliferation of CC by sponging miR-155-5p. pcDNA3.1-circ_0000337-induced downregulation of miR-155-5p level is rescued by miR-155-5p mimic (A), si-circ_0000337-induced upregulation of miR-155-5p level is attenuated by miR-155-5p inhibitor (B). pcDNA3.1-circ_0000337-induced facilitation of C33A cell proliferation is attenuated by miR-155-5p mimic (C), si-circ_0000337-induced repression of HeLa cell proliferation is partially reversed by miR-155-5p inhibitor (D). * $p < 0.05$, ** $p < 0.01$, *** $p < 0.001$ vs. NC, si-NC. # $p < 0.05$, ## $p < 0.01$, vs. circ_0000337, si-circ_0000337

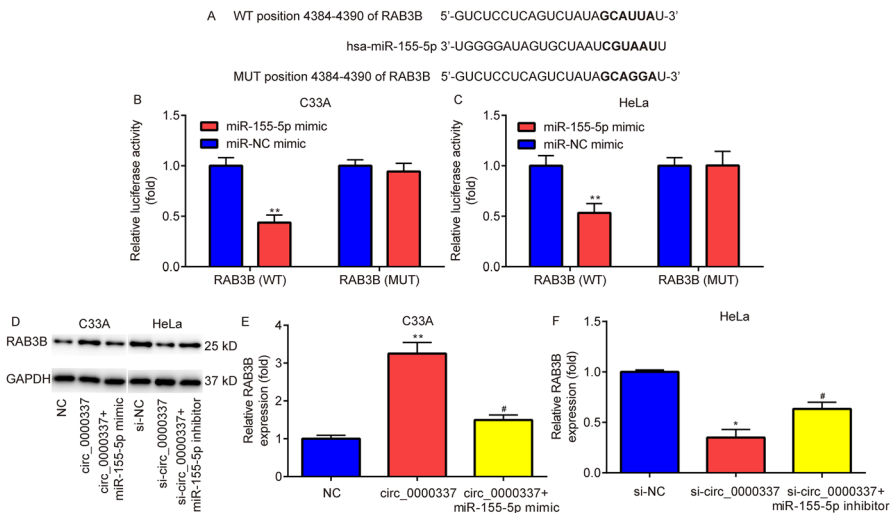


Fig. 7 circ_0000337 targets miR-155-5p to upregulate RAB3B expression. RAB3B is predicted as one of the potential mRNA targets of miR-155-5p (A). miR-155-5p mimic diminishes the luciferase activity of WT RAB3B but not MUT RAB3B in C33A (B) and HeLa (C). pcDNA3.1-circ_0000337 enhances RAB3B expression in C33A cells, which is attenuated by miR-155-5p mimic (D and E), si-circ_0000337 impedes RAB3B expression in HeLa cells, which is counteracted by miR-155-5p inhibitor (D and F). * $p < 0.05$, vs. si-NC, ** $p < 0.01$, vs. miR-NC mimic, NC. # $p < 0.05$, vs. circ_0000337, si-circ_0000337

RAB3B is Negatively Correlated with miR-155-5p, While Positively Correlated with circ_0000337

GEPIA demonstrates that RAB3B expression is upregulated in CESC tissues contrast to normal tissues (Fig. 8A). Consistently, RAB3B mRNA is overexpressed in CC cell lines relative to H8 (Fig. 8B), meanwhile, RAB3B mRNA is overexpressed in CC tissues in comparison with the adjacent non-cancerous tissues (Fig. 8C).

Notably, in CC tissues, RAB3B mRNA expression is negatively correlated with miR-155-5p expression (Fig. 8D), while positively correlated with circ_0000337 expression (Fig. 8E). Altogether, there is an inverse correlation between RAB3B and miR-155-5p, additionally, there is a positive correlation between RAB3B and circ_0000337.

RAB3B is Negatively Correlated with OS, While miR-155-5p is Positively Correlated with OS

Moreover, UALCAN (Fig. 9A) and Kaplan-Meier Plotter (Fig. 9B) indicates that high miR-155-5p expression is correlated with prolonged OS, while Kaplan-Meier Plotter (Fig. 9C), GEPIA (Fig. 9D), and ENCORI (Fig. 9E) demonstrates that low RAB3B expression is correlated with prolonged OS. Moreover, ENCORI shows that there is also a negative correlation between RAB3B and miR-155-5p (Fig. 9F). In sum, RAB3B expression shortens OS, while miR-155-5p expression prolongs OS of patients with CC.

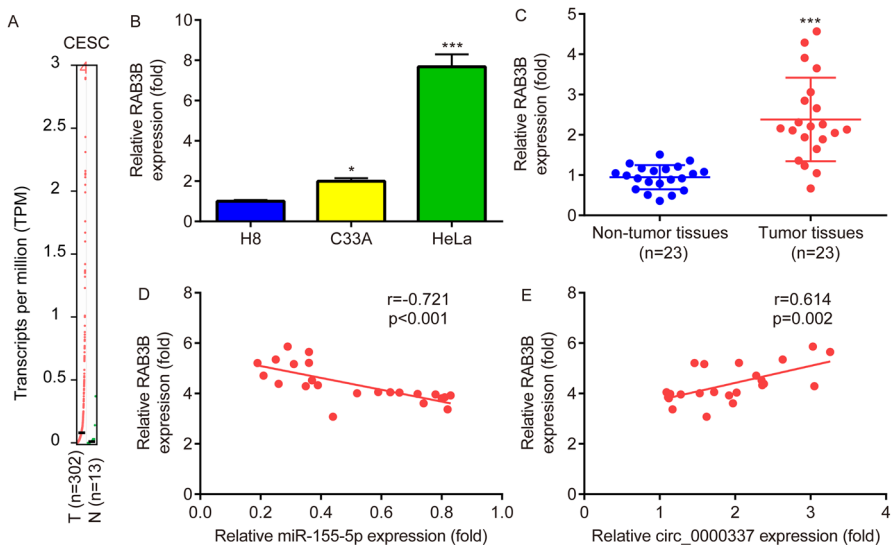


Fig. 8 RAB3B is negatively correlated with miR-155-5p, while positively correlated with circ_0000337. GEPIA demonstrates that RAB3B expression is upregulated in CESC tissues contrast to normal tissues (A). RAB3B mRNA is overexpressed in CC cell lines (B) and tumor tissues (C) relative to H8 and the adjacent non-cancerous tissues, respectively. RAB3B is negatively correlated with miR-155-5p (D), while positively correlated with circ_0000337 (E). * $p < 0.05$ vs. H8, *** $p < 0.001$ vs. non-tumor tissues, H8

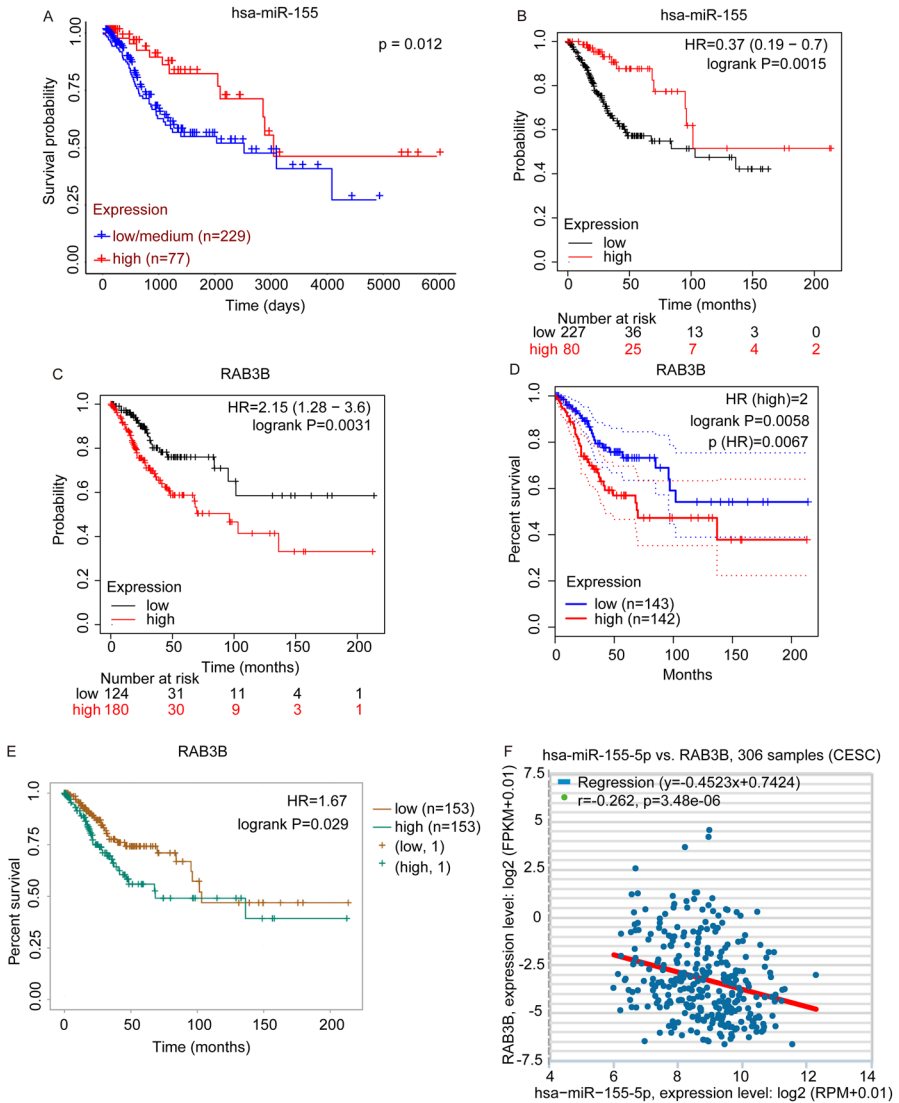


Fig. 9 RAB3B is negatively correlated with OS, while miR-155-5p is positively correlated with OS. UALCAN (A) and Kaplan-Meier Plotter (B) indicate that high miR-155-5p expression is correlated with prolonged OS. Kaplan-Meier Plotter (C), GEPIA (D), and ENCORI (E) demonstrate that low RAB3B expression is correlated with prolonged OS. ENCORI shows that there is a negative correlation between RAB3B and miR-155-5p (F)

Discussion

CircRNAs are novel endogenous non-coding RNAs which are implicated in cellular processes and regulate gene expression transcriptionally or post-transcriptionally by interacting with miRNAs or other molecules (Yang et al. 2017). Current study

focuses on the roles of circ_0000337 in the pathogenesis of CC, and demonstrates that circ_0000337 is highly expressed in the CC tissues and cells. Circ_0000337 overexpression facilitates cell proliferation, while circ_0000337 knock down restrains cell proliferation of CC cells. In support of the findings about the implication of circ_0000337 in the progression of CC, recent studies have shown that circ_0072995 drives CC development by targeting miR-29a/WDR5 axis (Song and Li 2022), circ_0001495 promotes CC progression by regulating miR-526b-3p/TMBIM6/mTOR axis (Zhang and Zheng 2022), circ_0000745 contributes to the progression of CC by targeting miR-409-3p/ATF1 axis (Cui et al. 2022).

A large quantity of RNA transcripts including lncRNAs, and circRNAs function as ceRNA of miRNAs and are implicated in numerous human diseases (Tay et al. 2014). Herein, circ_0000337 is verified to serve as a ceRNA of miR-155-5p. miR-155-5p is expressed at a low level in CC specimens relative to non-cancerous specimens, and is negatively correlated with circ_0000337. Bioinformatic analysis indicates that high miR-155-5p expression is related with prolonged OS of patients with CC. Altogether, the findings indicate the tumor suppressive role of miR-155-5p in CC, which is in consistent with a previous study showing that, in HPV+ human cervical lesion tissues, miR-155-5p expression was decreased; and compared to C33A (HPV-), miR-155-5p expression was lower in SiHa (HPV+) and HeLa (HPV+) (Wang et al. 2018).

Last but not least, RAB3B is found to be expressed at a high level for the first time in CC specimens and cell lines relative to non-cancerous specimens and normal cervical epithelial cells, respectively. circ_0000337 serves as a sponge of miR-155-5p to upregulate RAB3B. Furthermore, RAB3B is negatively correlated with miR-155-5p, while positively correlated with circ_0000337 in CC specimens. Meanwhile, high RAB3B expression is correlated with poor OS of patients with CC. Altogether, the findings indicate the onco-genetic role of RAB3B in CC, which was in line with a study showing that RAB3B in the circRNA-miRNA-mRNA network is negatively associated with OS, and RAB3B serves as a prognostic biomarker for patients with CC (Xu et al. 2020).

Conclusion

Collectively, the findings identify a circ_0000337/miR-155-5p/RAB3B regulatory axis where circ_0000337 upregulates RAB3B by sponging miR-155-5p to promote CC cell proliferation. Altogether, the present study highlighted the promising potential of circ_0000337 as a novel target for CC treatment.

Author Contributions All authors contributed to the study conception, study design, material preparation, data collection and analysis. The first draft of the manuscript was written by YH and all authors commented on previous versions of the manuscript. All authors read and approved the final manuscript.

Funding The present study is funded by Jiangsu Province Maternal and Children Health Research Project (F202139), Nantong Health Commission Research Project (MA2021015), Scientific Research and Innovation Team Project of Kangda College of Nanjing Medical University (KD2022KYCXTD010), State Key Laboratory of Oncogenes and Related Genes Research Project (KF2201).

Data Availability Data cannot be available due to they are also correlated with our another ongoing work.

Declarations

Competing interests The authors declare no competing interests.

Ethics Approval Current study was performed in line with the principles of the Declaration of Helsinki, and approved by the Ethics Committee of Affiliated Hospital 2 of Nantong University.

Consent to Participate Informed consent was obtained from all individual participants included in the study.

Consent to Publish The authors affirm that human research participants provided informed consent for publication of the images in Figs. 1a, 2, 5b and c and 8c, d and e.

References

- Arnaiz E, Sole C, Manterola L, Iparraguirre L, Otaegui D, Lawrie CH (2019) CircRNAs and cancer: biomarkers and master regulators. *Semin Cancer Biol* 58:90–99
- Cancer Genome Atlas Research Network, Analytical Biological Services (2017) Integrated genomic and molecular characterization of cervical cancer. *Nature* 543:378–384
- Chen LL (2016) The biogenesis and emerging roles of circular RNAs. *Nat Rev Mol Cell Biol* 17:205–211
- Chen B, Huang S (2018) Circular RNA: an emerging non-coding RNA as a regulator and biomarker in cancer. *Cancer Lett* 418:41–50
- Cohen PA, Jhingran A, Oaknin A, Denny L (2019) Cervical cancer. *Lancet* 393:169–182
- Cui X, Chen J, Zheng Y, Shen H (2022) Circ_0000745 promotes the progression of cervical cancer by regulating miR-409-3p/ATF1 axis. *Cancer Biother Radiopharm* 37:766–778
- Fader AN (2018) Surgery in Cervical Cancer. *N Engl J Med* 379:1955–1957
- Fang Y, Long F (2020) Circular RNA circ_0000337 contributes to osteosarcoma via the miR-4458/BACH1 pathway. *Cancer Biomark* 28:411–419
- Han B, Chao J, Yao H (2018) Circular RNA and its mechanisms in disease: from the bench to the clinic. *Pharmacol Ther* 187:31–44
- Jeck WR, Sharpless NE (2014) Detecting and characterizing circular RNAs. *Nat Biotechnol* 32:453–461
- Jhamad S, Aanjanee R, Jaiswal S, Jain S, Bhagat P (2018) Second primary cancer after radiotherapy for cervical cancer. *J Midlife Health* 9:207–209
- Li S, Teng S, Xu J, Su G, Zhang Y, Zhao J, Zhang S, Wang H, Qin W, Lu ZJ, Guo Y, Zhu Q, Wang D (2019) Microarray is an efficient tool for circRNA profiling. *Brief Bioinform* 20:1420–1433
- Liu NZ, Li T, Liu CM, Liu FR, Wang YX (2020) Hsa_circ_0000337 promotes proliferation, migration and invasion in glioma by competitively binding miRNA-942-5p and thus upregulates MAT2A. *Eur Rev Med Pharmacol Sci* 24:12251–12257
- Scheffe JH, Lehmann KE, Buschmann IR, Unger T, Funke-Kaiser H (2006) Quantitative real-time RT-PCR data analysis: current concepts and the novel gene expression's CT difference formula. *J Mol Med (Berl)* 84:901–910
- Shang C, Li Y, He T, Liao Y, Du Q, Wang P, Qiao J, Guo H (2021) The prognostic miR-532-5p-correlated ceRNA-mediated lipid droplet accumulation drives nodal metastasis of cervical cancer. *J Adv Res* 37:169–184
- Siegel RL, Miller KD, Jemal A (2019) Cancer statistics, 2019. *CA Cancer J Clin* 69:7–34
- Song Z, Li H (2022) Circ_0072995 drives cervical cancer development by regulating the miR-29a/WDR5 axis. *J Obstet Gynaecol* 42:3342–3348
- Song H, Xu D, Shi P, He B, Li Z, Ji Y, Agbeko CK, Wang J (2019) Upregulated circ RNA hsa_circ_0000337 promotes cell proliferation, migration, and invasion of esophageal squamous cell carcinoma. *Cancer Manag Res* 11:1997–2006
- Tay Y, Rinn J, Pandolfi PP (2014) The multilayered complexity of ceRNA crosstalk and competition. *Nature* 505:344–352
- Wang F, Shan S, Huo Y, Xie Z, Fang Y, Qi Z, Chen F, Li Y, Sun B (2018) MiR-155-5p inhibits PDK1 and promotes autophagy via the mTOR pathway in cervical cancer. *Int J Biochem Cell Biol* 99:91–99
- Wilting SM, Snijders PJ, Verlaet W, Jaspers A, van de Wiel MA, van Wieringen WN, Meijer GA, Kenter GG, Yi Y, le Sage C, Agami R, Meijer CJ, Steenbergen RD (2013) Altered microRNA expression associated with chromosomal changes contributes to cervical carcinogenesis. *Oncogene* 32:106–116

- Xu T, Song X, Wang Y, Fu S, Han P (2020) Genome-wide analysis of the expression of circular RNA full-length transcripts and construction of the circRNA-miRNA-mRNA network in cervical cancer. *Front Cell Dev Biol* 8:603516
- Yang Z, Xie L, Han L, Qu X, Yang Y, Zhang Y, He Z, Wang Y, Li J (2017) Circular RNAs: regulators of cancer-related signaling pathways and potential diagnostic biomarkers for human cancers. *Theranostics* 7:3106–3017
- Yu DS, Song XL, Yan C (2021) Oncogenic miRNA-1908 targets HDAC10 and promotes the aggressive phenotype of cervical cancer cell. *Kaohsiung J Med Sci* 37:402–410
- Zang R, Qiu X, Song Y, Wang Y (2021) Exosomes mediated transfer of Circ_0000337 contributes to cisplatin (CDDP) resistance of esophageal cancer by regulating JAK2 via miR-377-3p. *Front Cell Dev Biol* 9:673237
- Zhang X, Zheng X (2022) Hsa_circ_0001495 contributes to cervical cancer progression by targeting miR-526b-3p/TMBIM6/mTOR axis. *Reprod Biol* 22:100648

Publisher's Note Springer Nature remains neutral with regard to jurisdictional claims in published maps and institutional affiliations.

Springer Nature or its licensor (e.g. a society or other partner) holds exclusive rights to this article under a publishing agreement with the author(s) or other rightsholder(s); author self-archiving of the accepted manuscript version of this article is solely governed by the terms of such publishing agreement and applicable law.

Authors and Affiliations

Jiqin Xu¹ · Bai Xue¹ · Min Gong¹ · Ling Ling¹ · Sipei Nie¹ · Fujun Li¹ · Meixia Wang² · Miao Fang¹ · Chen Chen³ · Qiaoling Liu¹ · Yun Han^{3,4}

✉ Qiaoling Liu
1134447805@qq.com

✉ Yun Han
hanyun_888@163.com

¹ Department of Obstetrics and Gynecology, Nanjing Jiangning Hospital Affiliated to Nanjing Medical University, No. 169 Hushan Road, Nanjing 211100, Jiangsu, China

² Department of Gynaecology and Obstetrics, Wenzhou Hospital of Integrated Traditional Chinese and Western Medicine, Wenzhou 325000, Zhejiang, China

³ Department of Obstetrics and Gynecology, Affiliated Hospital 2 of Nantong University, No. 666 Shengli Road, Nantong 226000, Jiangsu, China

⁴ State Key Laboratory of Systems Medicine for Cancer, Shanghai Cancer Institute & Renji Hospital Affiliated to Shanghai Jiao Tong University School of Medicine, No. 227 South Chongqing Road, Shanghai 200025, China